Journal of the Serbian Chemical Society
JSCS-info@shd.org.rs • www.shd.org.rs/JSCS
J. Serb. Chem. Soc. *82* (3) 303–316 (2017)
JSCS–4967
UDC 547.53.024'442+547.841'264:
66.094.1.004.12:544.362
Original scientific paper

Redox properties of alkyl-substituted 4-aryl-2,4-dioxobutanoic acids

ILIJA N. CVIJETIĆ[1], TATJANA Ž. VERBIĆ[2]*, BRANKO J. DRAKULIĆ[3]**, DALIBOR M. STANKOVIĆ[1,4#], IVAN O. JURANIĆ[3], DRAGAN D. MANOJLOVIĆ[2] and MIRE ZLOH[5]

[1]Innovation Center of the Faculty of Chemistry, University of Belgrade, Studentski trg 16, 11000 Belgrade, Serbia, [2]Faculty of Chemistry, University of Belgrade, Studentski trg 16, 11000 Belgrade, Serbia, [3]Institute of Chemistry, Technology and Metallurgy, Department of Chemistry, University of Belgrade, Njegoševa 12, 11000 Belgrade, Serbia, [4]Vinča Institute of Nuclear Sciences, University of Belgrade, P. O. Box 522, 11001 Belgrade, Serbia and [5]Department of Pharmacy, University of Hertfordshire, Hatfield, Hertfordshire AL10 9AB, United Kingdom

(Received 23 November 2016, revised 4 February, accepted 7 February 2017)

Abstract: Redox properties of a set of aryldiketo acids (ADKs), small organic molecules that comprise 2,4-dioxobutanoic acid moiety, were studied. Along with well-known HIV-1 integrase (IN) inhibition, ADKs exert widespread biological activities. The aim of this work was to evaluate the effects of aryl substitutions on the properties of the dioxobutanoic moiety that is involved in key interactions with metal ions within the active sites of target enzymes. The effect of pH on the electronic properties of nine congeners was examined using cyclic voltammetry and differential pulse polarography. The compounds were chosen as a simple set of congeners bearing Me-groups on the phenyl ring, which should not be involved in electrochemical reactions, leaving the diketo moiety as the sole electrophore. The substitution pattern was systematically varied, yielding a set having different torsion between the phenyl ring and the aryl keto group (Ar–C(O)). The protonation state of the ADKs at different pH values was determined from the experimentally obtained pK_a values. The results showed that an equal number of protons and electrons were involved in the oxidation and reduction reactions at the surface of the electrode. Quantitative linear correlations were found between the reduction potentials and the energies of the frontier orbitals, calculated for neutral, mono-anionic and the corresponding radical anionic species, and the steric parameter as two independent variables.

* Corresponding author. E-mail: tatjanad@chem.bg.ac.rs
** Authors regret to inform that Branko Drakulić has passed away since completion of this paper.
# Serbian Chemical Society member.
doi: 10.2298/JSC161118021C

Keywords: aryldiketo acids (ADKs); redox properties; structure–property relationship; acidity constants.

INTRODUCTION

Small organic molecules that comprise 2,4-dioxobutanoic acid moiety in their structures exert widespread biological activities along with their well-known HIV-1 integrase (IN) inhibition.[1–3] Such compounds were described as inhibitors of: the HIV-1 reverse transcriptase ribonuclease H domain (RT – RNase H);[4] undecaprenyl diphosphate synthase, the enzyme involved in bacterial cell wall biosynthesis;[5] *M. tuberculosis* malate synthase,[6] the endonuclease activity of the La Crosse orthobunyavirus L-protein;[7] the influenza virus PA endonuclease;[8–10] the duplex DNA-unwinding activity of the SARS coronavirus NTPase/helicase;[11] the protein tyrosine phosphatase 1B;[12] bacterial aldolases;[13] the hepatitis C virus RNA-dependent RNA polymerase,[14] and as inhibitors of protein–protein interactions between HIV-1 integrase and the cellular cofactor LEDGF/p75.[15] It was shown that 4-aryl-2,4-dioxobutanoic acids (aryldiketo acids, ADKs) exert promising activity against multidrug resistant bacteria.[16]

Herein, as a continuation of work on structure–property relationship studies[17,18] and the biological activity of ADKs,[16] the effects of pH on electronic properties of nine congeners (compounds **1**–**9**, Fig. 1) were investigated using cyclic voltammetry (CV), and differential pulse polarography (DPP). Compounds **1**–**9** were chosen as a simple set of congeners, bearing Me-groups that should not be involved in electrochemical reactions to evaluate the effects of aryl substitution on the dioxobutanoic moiety. It was shown that this moiety is responsible for the inhibitory activity of ADKs since it is involved in interactions with metal ions within active sites of target enzymes.[18] The substitution pattern on the phenyl ring was systematically varied, yielding a set having different torsion between phenyl ring and the aryl keto group (Ar–C(O)). Due to the presence of *ortho*-Me groups and tri- and tetra-Me-substitution at the phenyl ring for some compounds, different congeners most probably differently approach and interact with the electrode.

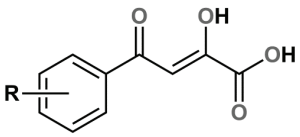

R = H (comp.**1**); 2-CH_3 (**2**); 3-CH_3 (**3**); 4-CH_3 (**4**); 2,4-di-CH_3 (**5**); 2,5-di-CH_3 (**6**); 3,4-di-CH_3 (**7**); 2,4,5-tri-CH_3 (**8**); 2,3,5,6-tetra-CH_3 (**9**)

Fig. 1. Structures of methyl-substituted ADKs studied within this work.

There are many electrochemical studies of various 1,3-diketones and their metal complexes in the literature.[19–22] Nevertheless, except data on the polaro-

graphic behavior of four aryldiketo acid methyl-esters (unsubstituted, 4-Me-Ph, 4-Cl-Ph and 2-HO-Ph) in the pH range 2–12 in aqueous 20 % 2-propanol,[23] to the best of our knowledge there are no similar reports for ADKs. Oxidation and reduction potentials of the compounds at pH 1, 5 and 10, as well as the pK_a values of the carboxyl group and the hydroxy group in the α-position with respect to carboxyl group were experimentally obtained. ADKs could simultaneously exist in two enol forms (**I** and **III**), conformationally locked (through intramolecular hydrogen bonding) by the pseudo-ring, and one diketo form (**II**) having two rotatable bonds, responsible for their conformational mobility (Fig. 2).[24,25]

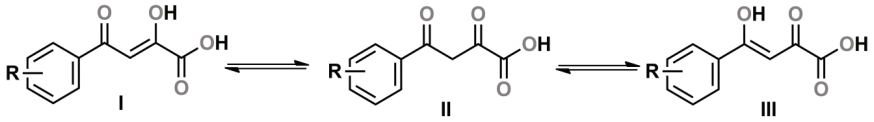

Fig. 2.Tautomerism of aryldiketo acids; two enol forms (**I** and **III**) and one diketo form (**II**).

From the NMR spectra of compound **1** recorded in the pH range 1 to 10, it was concluded that enol form **I** is predominant in aqueous solutions over a wide pH range,[26] and hence, for all calculations, the enol form **I** of the molecules was chosen. The geometries of the molecules in their neutral, monoanionic and corresponding radical anion or cation forms were optimized by MP2 calculations using the 6-31G(d,p) basis set.

EXPERIMENTAL

Reagents and apparatus

All chemicals were purchased from Fluka, Aldrich, or Merck, having >98 % purity, and were used as received. For purity assessment of the compounds, methanol (Merck, LiChrosolv), HCOOH (Fisher Scientific, F/1750/PB15), and acetonitrile (Sigma–Aldrich, Chromasolv) were used. For the thin-layer chromatography, silica gel pre-coated plates with fluorescent indicator (254 nm) were used.

Melting points were determined in open capillary tubes on a Stuart SMP-10 instrument and are uncorrected. The ESI-MS analysis was performed in methanol on an Agilent Technologies 6210-1210 TOF-LC-ESI-MS instrument in the negative mode. The IR spectra were recorded on a Thermo Nicolet 6700 FT-IR spectrometer equipped with an ATR accessory. The ^{1}H- and ^{13}C-NMR spectra of compounds **1**–**9** were recorded in DMSO-d_6, $CDCl_3$ or CD_3OD on a Varian Gemini 2000 200/50 MHz or a Bruker Avance 500/125 MHz NMR instruments. Multiplicities are reported as: *s* (singlet), *bs* (broad singlet), *d* (doublet) and *t* (triplet). All coupling constants (*J*) are given in Hz. Chemical shifts are given in ppm, relative to the solvent signals. Purity of compounds was analyzed by HPLC on an Agilent Technologies 1260 Infinity Series instrument equipped with a Zorbax Eclipse XDB-C18 (4.6 mm×50 mm, 1.8 μm) column. Physical, analytical and spectral data of the compounds are given in Supplementary material to this paper.

Cyclic voltammograms were recorded using a CHI760B instrument (CH Instruments, USA). The cell was equipped with a glassy carbon electrode and an accessory Pt electrode (model CHI221, cell top including the Pt wire counter electrode) and an Ag/AgCl reference

electrode (model CHI111). Differential pulse polarograms were recorded using a Metrohm 797 VA COMPUTRACE (Netherlands). The electrochemical cell was equipped with a dropping mercury electrode, Ag/AgCl (3 M KCl) reference electrode, and platinum wire as the accessory electrode.

For the determination of the acidity constants, UV/Vis spectra were recorded on a GBC Cintra 6 spectrophotometer (GBC Dandenong, Australia) with 1 cm quartz cuvette. The pH values were measured using a CRISON pH-Burette 24 2S, equipped with CRISON 50 29 micro-combined pH electrode (Crison Instruments, S.A. Spain). The electrode was calibrated by standard CRISON buffer solutions (pH 4.01, 7.00, and 9.21).

*Synthesis and characterization of compounds **1**–**9***

The compounds were prepared by addition of equimolar amounts of Ph-substituted acetophenones and diethyl oxalate to a twofold molar amount of sodium methoxide, obtained by dissolution of sodium in dry MeOH. The reaction mixture was stirred overnight, then poured into ice-cold water and vigorously stirred for additional ≈3 h at room temperature. Subsequently, the reaction mixture was filtered into water acidified with hydrochloric acid to pH 2–3. The obtained precipitate was collected by filtration and washed by ice-cold water. Evaporation of MeOH from filtrate leads to the precipitation of additional amount of products. The crude products were recrystallized from appropriate solvents.

The physical, analytical and spectral data of compounds **1**–**9** are given in the Supplementary material to this paper.

HPLC determination of the purity of the compounds

Stock solutions of compounds **1**–**9**, 2 mg mL^{-1} were prepared in methanol, and 1 μL was injected onto the column. Gradient elution was performed in the following steps: 0–1 min, 100 % solvent A; 1–6 min, linear gradient from 100 % A to 0 % A (100 % B); 6–12 min, 100 % B. Solvent A: 0.2 % HCOOH in water; Solvent B: acetonitrile. The obtained chromatograms are shown in the Supplementary material, Figs. S-1–S-9.

Electrochemistry

Britton–Robinson buffers (pH range 1–10) were used for all measurements. Cyclic voltammograms were recorded on a glassy carbon electrode (GCE) at a scan speed 100–500 mV s^{-1}. All differential pulse voltammograms were recorded at a scan speed 13 mV s^{-1} (pulse amplitude 50 mV and pulse time 0.4 s). Nitrogen was bubbled for 200 s before each measurement.

Acidity constants determination

The acidity constants were spectrophotometrically determined at $t = 25\pm1$ °C and constant ionic strength 0.1 M (NaCl). Stock solutions were prepared in ethanol ($c = 1\times10^{-2}$ M); working solutions ($c = 1\times10^{-4}$ M) were prepared in deionized water (the ethanol concentration was 1 vol. %) in the pH ranges 1.0–3.5 for pK_{a1} and 6.1–9.8 for pK_{a2}, solutions of HCl were used for pH 1.0–3.5, phosphate buffers for pH 6.1–8.0 ($c_{tot} = 0.01$ M), and carbonate buffers for pH 8.0–9.8 ($c_{tot} = 0.01$ M). The UV/Vis spectra of the monoanionic form (HA^-) of the ADKs were recorded in acetate buffer ($c_{tot} = 0.01$ M, pH 4.5–5.0). The spectra were recorded over the 220–500 nm wavelength range at a scanning speed of 500 nm min^{-1} against the appropriate HCl or buffer solution as the corresponding blank. The absorbances were measured at the wavelength of the absorption maximum or at the wavelength of the maximal differences in the absorbances. Three sets of experiments were performed. The values of the

acidity constants were determined according to two transformed forms of the classical spectrophotometric equation:[27]

$$A = A_{H_2A} - K_{a1}\frac{A - A_{HA^-}}{[H_3O^+]} \quad (1)$$

$$A = A_{A^{2-}} + \frac{1}{K_{a2}}[H_3O^+](A_{HA^-} - A) \quad (2)$$

where A_{H_2A}, A_{HA^-}, $A_{A^{2-}}$, and A represent the absorbances of molecular (H_2A), monoanionic (HA^-), dianionic (A^{2-}) forms of the ADKs and their mixture at specified wavelengths, respectively. Equations (1) and (2) gave linear dependences where the spectrum of only one "pure" form (HA^-) was needed for K_{a1} and K_{a2} determination. The values of K_{a1} and K_{a2} were calculated by linear regression analysis from the slope of the corresponding fitting line (Supplementary material, Figs. S-10–S-21). The determination of the pK_a values of compounds **1**, **4** and **7** was previously described.[17]

Calculations setup

The full geometry optimizations of compounds **1**–**9** in their neutral (H_2A) and anionic forms (HA^-) were performed at the MP2 level of theory using the 6-31G(d,p) basis set. The geometries and energies of the H_2A and HA^- forms of **1**–**9** are given in the Supplementary material, Figs. S-22 and S-23. The influence of solvent was simulated applying the implicit (water) solvation model, IEF-PCM. The energies of the radical anions and radical cations of the H_2A form, and the radical anions of the HA^- form of the compounds were obtained by single-point calculations from the optimized geometries of H_2A or HA^-. The enol form **I** of compounds **1**–**9** was used, and appropriate charges and spin multiplicities in input files were chosen. All calculations were performed in the Gaussian09 program.[28]

RESULTS AND DISCUSSION

Identity and purity of compounds **1**–**9**, synthesized according to previously reported procedure,[29] was confirmed using ^{1}H-, ^{13}C-NMR and IR spectroscopy, melting point determination, high resolution MS and HPLC analysis (Supplementary material). All compounds had > 95 % purity, as confirmed by HPLC.

The spectrophotometrically determined values of the acidity constants (pK_a) of the compounds are given in Table I. The distribution diagram of H_2A, HA^-, and A^{2-} forms of compound **1** are shown in Fig. 3. The pK_{a1} values stands for the acidity constant of ADKs' carboxyl group and the pK_{a2} for the acidity constant of enol –OH group. In aqueous media, ADKs act as diprotic acids sparingly soluble in water, with the lowest solubility in acidic media (at pH < pK_{a1}), where they are mostly present in the molecular, *i.e.*, unionized, form (H_2A).

As a trend, lower pK_a values were observed for the *ortho*-substituted derivatives, with compound **9** being the most acidic one, most probably due to the presence of two *ortho*-substituents. Hyperchromic and blue shifts of UV/Vis absorption maxima of the ADKs with increasing pH value was also observed (Figs. S-10–S-21 of the Supplementary material), which could be attributed to the increased electron density of the chromophore.

TABLE I. Spectrophotometrically determined pK_a values of compounds **1**–**9** (I = 0.1 M (NaCl), t = 25±1 °C)

Compound	pK_{a1}±*SD*	pK_{a2}±*SD*
1	2.06±0.03[a]	7.56±0.02[a]
2	2.11±0.01	6.94±0.04
3	2.27±0.06	7.52±0.02
4	2.22±0.05[a]	7.99±0.02[a]
5	2.02±0.04	7.28±0.04
6	2.39±0.04	7.23±0.04
7	2.09±0.04[a]	7.92±0.04[a]
8	2.18±0.04	6.79±0.06
9	1.96±0.04	6.50±0.05

[a]Previously published[17] pK_a values

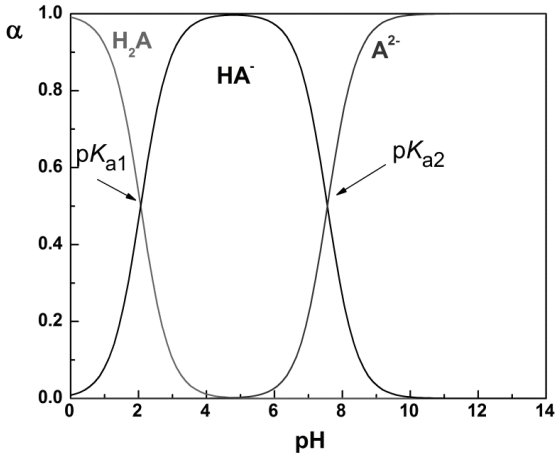

Fig. 3. Protonation states of compound **1** at pH values 0 to 14.

CV and DPP were used to examine the electrochemical behavior of the studied compounds at three pH values, *i.e.*, 1, 5 and 10. In this way, the electrochemical properties of neutral, monoanionic and dianionic forms of the compounds were covered.

Representative cyclic voltammograms (CVM) of the pure H_2A, HA^- and A^{2-} forms and the $E = f$(pH) dependence for compound **4** are shown in Fig. 4a. The peak potentials for all compounds are given in Table II and the CVM are given in the Supplementary material, Fig. S-24.

All compounds showed only one anodic (oxidation) peak at pH 1. The involvement of protons and electrons in oxidation within pH range 1–4 was determined according to the shift of peak potential as a function of pH (Fig. 4b). The obtained slope (–0.052±0.002 V pH^{-1}) was close to Nernstian, indicating that the electrode reaction involves an equal number of protons and electrons within pH range 1–4. Therefore, the oxidation of the ADKs is one-electron process involving the loss of one proton (most probably from the carboxyl group).

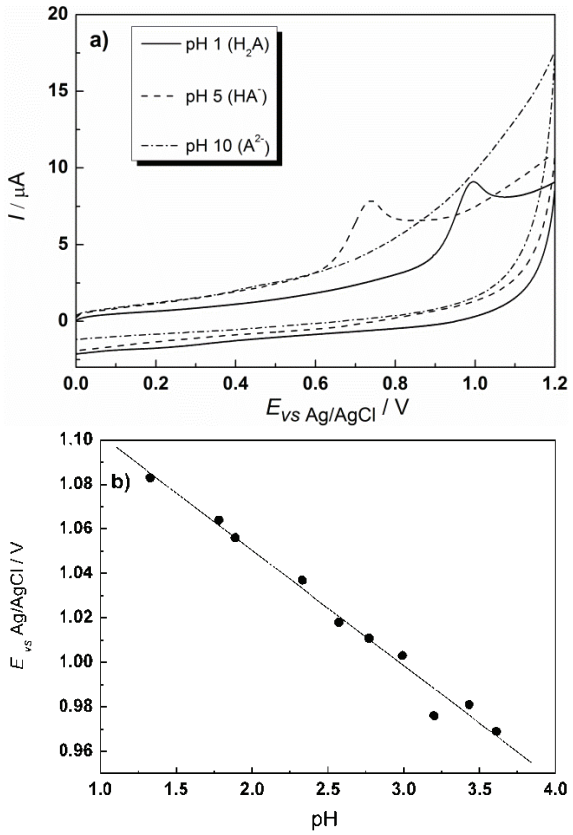

Fig. 4. a) Cyclic voltammograms of compound **4** in Britton–Robinson buffer at pH 1, 5 and 10; b) E = = f(pH) dependence for compound **4**, $E = a + b$pH, a = (1.154±0.006) V, b = (–0.052±0.002) V, r^2 = = 0.992; ($c_4 = 4.77 \times 10^{-5}$ M, scan rate 100 mV s^{-1}, t = 25±1 °C).

TABLE II. Oxidation and reduction potentials (E, given in V) of compounds **1**–**9** in Britton–Robinson buffer, at pH 1, 5, and 10, and the numerical values of the indicator variable (I)

Compound	E_{ox}, pH 1	E_{ox}, pH 5	E_{ox}, pH 10	E_{red}, pH 1	E_{red}, pH 5	I
1	1.008	0.717	Not observed	–0.5296	–0.7974	0
2	1.004	0.744	0.568	–0.5415	–0.7855	1
3	0.994	0.748	0.625	–0.5296	–0.7736	1
4	0.993	0.737	Not observed	–0.5475	–0.8093	0
5	0.997	0.750	0.514	–0.5534	–0.7915	1
6	0.996	0.736	0.520	–0.5475	–0.7617	2
7	1.005	0.751	0.444	–0.5534	–0.7796	1
8	1.002	0.795	0.510	–0.5475	–0.7617	2
9	0.936	0.713	0.524	–0.4999	–0.7379	4

A reversible reduction peak was not observed at any of the tested scan rates (50–500 mV s^{-1}). The one-electron oxidation of the ADKs generated a radical cation that was not stable long enough to allow a reversible cathodic reaction, and hence, a concurrent chemical reaction (most likely polymerization) occurred. In the second CV cycle (Fig. 5), the current decreased due to strong adsorption of

studied compounds at the electrode surface. The adsorption of structurally similar molecules at the surface of glassy carbon electrode was described in the literature.[30,31] The oxidation of the ADKs was facilitated with increasing pH value (lower oxidation potentials) and, simultaneously, the peak current decreased, most probably due to stronger adsorption on the electrode surface. At pH 10, a negligible oxidation peak was observed for all compounds.

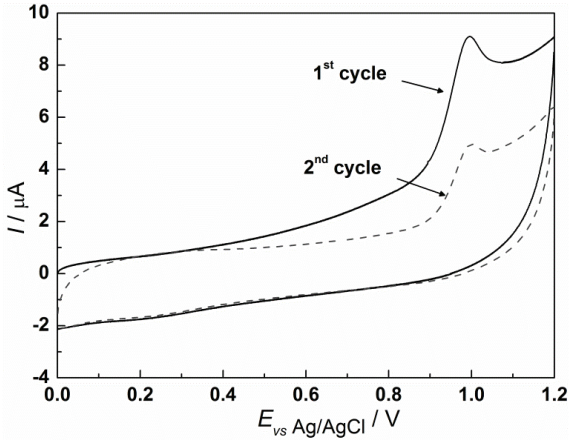

Fig. 5. Two CV cycles of compound **4** (c_4 = 4.77×10^{-5} M, scan rate 100 mV s^{-1}, t = 25±1 °C).

Since no reversible reduction peak was observed in the CV experiments, DPP on a dropping mercury electrode was used to study the reduction features of the compounds in aqueous medium within the pH range 1–10. Representative polarograms of the pure H_2A, HA^- and A^{2-} forms and $E = f$(pH) dependence for compound **1** are shown in Fig. 6a. Polarograms for all compounds are given in the Supplementary material, Fig. S-25. As the slope in $E = f$(pH) dependence (Fig. 6b) was close to Nernstian ((–0.058±0.002) V), the reduction appears to be a one-electron process.

As the pH value was increased, the reduction potential shifted to more negative values. At pH 10, no reduction peak was observed. Reduction potentials for all compounds at pH 1 and pH 5 are given in Table II.

Electrochemical oxidation and reduction are electron transfer processes between the electro-active molecule and the electrode surface. These heterogeneous processes are influenced by various effects beyond purely electronic ones, *i.e.*, it is well established that the way a molecule approaches the electrode and the nature of the electric double layer at the surface of the electrode affect electron transfer.[32] To obtain quantitative correlation between the oxidation and reduction potentials and structural features of compounds **1**–**9**, descriptors derived from *ab initio* calculations were used.

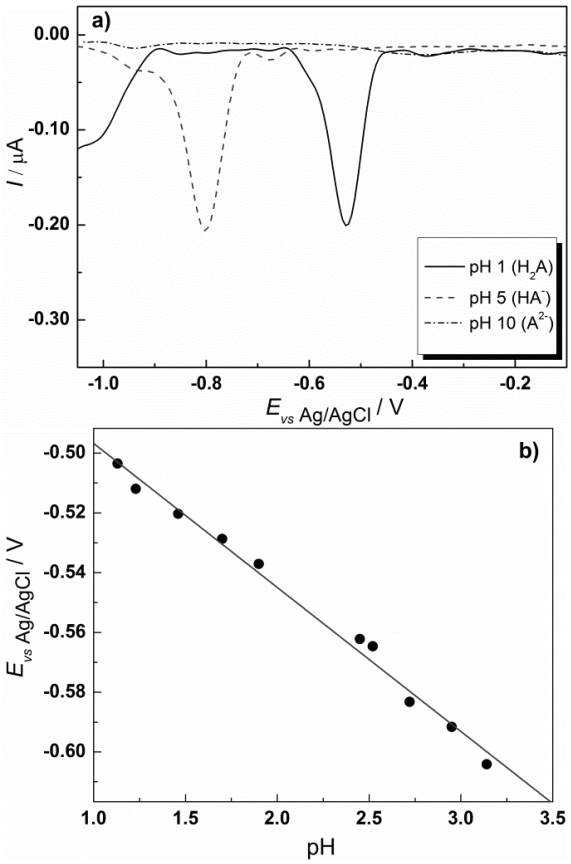

Fig. 6. Differential pulse polarograms of compound **1** in Britton–Robinson buffer at pH 1, 5 and 10; b) $E = f(\mathrm{pH})$ dependence for compound **1**, $E = a + b\mathrm{pH}$, a = (–0.538±0.005) V, b = (–0.058±±0.002) V, $r^2 = 0.995$; (c_1 = 5.46×10^{-5} M, scan rate 13 mV/s, t = 25±1 °C).

Frontier molecular orbitals, which describe the whole molecules and account for their reactivity, appear as a logical choice. As already noted, the enol form **I** was used and the geometry of all the studied compounds in their neutral forms was optimized. The electron density distribution of the HOMO and LUMO for representative compounds is shown in the Supplementary material, Figs. S-26 and S-27. The HOMO of all members of the set is located mainly on the phenyl ring while the corresponding LUMO electron density is generally located on the hydroxy-butanoic moiety. Upon removal of a hydrogen from the carboxyl group (deprotonation), the optimized structures were used as the input for full geometry optimization of the compounds in their monoanionic form. Subsequently, single point calculations were performed on the structures of the molecules optimized in their neutral forms to obtain αSOMO (singly occupied molecular orbital) and αLUMO energies for the radical cations and radical anions. Single point calculations on the fully optimized geometries of the monoanions (HA^- forms) were used to obtain the αSOMO and αLUMO energies for the radical dianions (radical

anions of the HA^- form). In all calculations, the implicit solvation model is used. The FMO energies and the corresponding gaps between those orbitals (HOMO––LUMO and *α*SOMO–*α*LUMO) of the neutral, anionic and corresponding radical forms of the compounds were included in the pool of descriptors, Tables S-I and S-II of the Supplementary material. The pool of descriptors was enhanced by the addition of the numeric values of molecular dipoles for all the studied forms (Tables S-I and S-II of the Supplementary material), and the indicator variable (*I*), which corresponds to number of *ortho*- and *meta*-alkyl substituents on the phenyl ring (Table II). From the optimized geometries of the molecules, it is clear that the Ar-to-C(O) torsion of the *ortho*-substituted compounds is larger than for the other compounds, due to repulsion of the *ortho*-Me and the aroyl--C(O)– moiety. Furthermore, alkyl substituents in *ortho*- and *meta*-positions most probably influence the approach and interaction of the molecules to the electrode. An attempt to include the square cosine values of the torsion angles between Ar and the –C(O)– moieties of the molecules, in order to provide a more precise description of the differences in the geometry, proved unproductive; such descriptor did not fit to any correlation (data not shown).

At pH 1, all compounds exist in the molecular, while at pH 5, all compounds are in their monoanionic form (Fig. 3, Table I). To make correlations of the redox potentials experimentally obtained at different pH values, descriptors derived from the optimized geometries of the corresponding forms were used. Descriptors derived for the neutral form of the molecules were used in the correlation with redox properties obtained at pH 1, while descriptors derived for the monoanionic forms were used for pH 5.

The intercorrelation matrix of the descriptors used (Table S-III of the Supplementary material) and the numeric values of the oxidation and reduction potentials revealed good correlations (r values > 0.9) between:

– E_{red}_pH_1 and the SOMO–LUMO gap for the radical anions;
– E_{ox}_pH_1 and the SOMO–LUMO gap for the radical cations;
– E_{ox}_pH_1 and the numerical values of the dipoles of the radical cations;
– E_{ox}_pH_5 and the numerical values of the dipoles of the radical cations.

Exclusion of derivative **9** resulted in statistically insignificant correlations in all instances.

Regarding two-parameter correlations, good linear relationships between the reduction potentials obtained at pH 5 and either the energy of the LUMO orbitals of the anions of the compounds (Eq. (3)), or the energy of the *α*LUMO orbitals of the radical dianions (obtained by the one-electron reduction of the HA^- forms) (Eq. (4)) and the indicator variable were found:

$$E_{red\_pH\_5} = (-3.059\pm1.170)E_{LUMO,anion} + \\ +(0.0275\pm0.0045)I - (0.610\pm0.073) \quad (3)$$

$$(n = 9;\ r = 0.994;\ s = 0.003;\ F = 253.878;\ Q^2 = 0.977;\ SD_{cv} = 0.004)$$

$$E_{red\_pH\_5} = (-0.905\pm0.780)E_{LUMO,radical\_dianion} + (0.0231\pm0.0064)I - (1.151\pm0.300) \quad (4)$$

$$(n = 9;\ r = 0.980;\ s = 0.005;\ F = 73.796;\ Q^2 = 0.709;\ SD_{cv} = 0.013)$$

Graphical presentations of the predicted *vs*. the experimental values, derived from Eqs. (3) and (4), are given in Fig. 7.

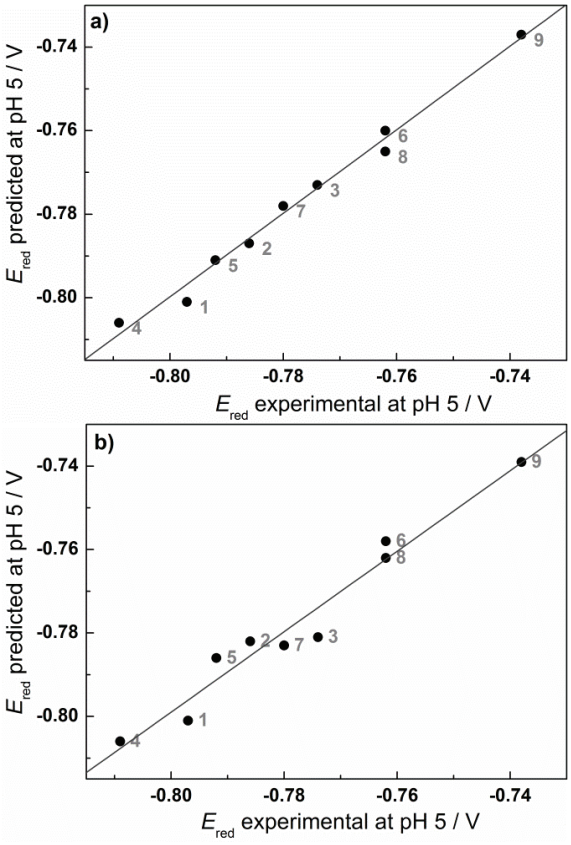

Fig. 7. Predicted *vs.* experimental reduction potentials at pH 5 derived using: a) Eq. (3); b) Eq. (4).

Similar correlations could be obtained with the difference between αSOMO and αLUMO for the radical anions and the indicator variable, but such correlations had significantly lower internal predictivity (Q^2 value, obtained by the leave-one-out cross-validation). Aside the good statistics in Eqs. (3) and (4), the very good correlation between the reduction potentials at pH 5 and the indicator variable alone ($r = 0.953$) should be noted.

If the normalized values of the variables are considered, the regression coefficients in Eqs. (3) and (4) revealed the importance of each term for the description of the reduction potentials. Although the indicator variable, accounting

for steric effects, featured in both correlations, the importance of FMO descriptors was somewhat higher. No statistically significant correlations could be found using any combination of descriptors for reduction potentials obtained at pH 1, nor for the oxidation potentials at pH 1 and pH 5. This may be due to adsorption of electro-oxidation products at the electrode, which was observed experimentally (Fig. 5).

CONCLUSIONS

In continuation of ongoing work on structure–property relationships and the biological activity of ADKs, the redox properties of nine congeners were measured at three pH values, where they are present in molecular, monoanionic or dianionic form, in CV and DPP experiments. The substitution pattern on phenyl ring of the examined compounds was systematically varied, yielding a set having different torsion between the phenyl ring and the aryl keto group (Ar--C(O)), to evaluate the effects of substituents on the dioxobutanoic moiety. Oxidation and reduction involved the same number of protons and electrons. The oxidation of ADK is a one-electron process involving the loss of one proton, while a reversible reduction peak was not observed. DPP measurements revealed shifts of reduction potential to more negative values with increasing pH. It was observed that *ortho*-substituted ADKs have lower pK_{a1} and pK_{a2} values compared to those of the other derivatives.

The optimized geometries of all the studied congeners were used to rationalize the results of the CV and DPP experiments. The influence of substituents on the electrochemical behavior of the ADKs was quantified using quantum chemical descriptors. Very good linear correlations between the reduction potentials determined at pH 5 and the calculated FMOs and a descriptor that accounts for steric effects were observed.

SUPPLEMENTARY MATERIAL

Physical, analytical and spectral data of the compounds, as well as additional experimental data, are available electronically at the pages of journal website: http://www.shd.org.rs/JSCS/, or from the corresponding author on request.

Acknowledgements. Ministry of Education, Science, and Technological Development of the Republic of Serbia supported this work, Grant No. 172035. This work was also supported by Magbiovin project (FP7-ERAChairs-PilotCall-2013, grant agreement: 621375). The authors gratefully acknowledge the computational time provided on the PARADOX cluster at the Scientific Computing Laboratory of the Institute of Physics, Belgrade, as well as the PhD student Miloš Pešić and the Petnica Science Center, Serbia, for the HPLC analysis.

ИЗВОД

РЕДОКС СВОЈСТВА АЛКИЛ-СУПСТИТУИСАНИХ 4-АРИЛ-2,4-ДИОКСОБУТАНСКИХ КИСЕЛИНА

ИЛИЈА Н. ЦВИЈЕТИЋ[1], ТАТЈАНА Ж. ВЕРБИЋ[2], БРАНКО Ј. ДРАКУЛИЋ[3], ДАЛИБОР М. СТАНКОВИЋ[1,4], ИВАН О. ЈУРАНИЋ[3], ДРАГАН Д. МАНОЈЛОВИЋ[2] и МИРЕ ЗЛОХ[5]

[1]Иновациони центар Хемијског факултета Универзитета у Београду, Студентски трг 16, Београд, [2]Универзитет у Београду – Хемијски факултет, Студентски трг 16, Београд, [3]ИХТМ, Центар за хемију, Универзитет у Београду, Његошева 12, Београд, [4]Институт за нуклеарне науке „Винча“, Универзитет у Београду, п. пр. 522, Београд и [5]Department of Pharmacy, University of Hertfordshire, Hatfield, Hertfordshire AL10 9AB, United Kingdom

У оквиру овог рада проучаване су особине неколико арилдикето киселина (ADK), једињења која спадају у групу 2,4-диоксобутанских киселина. Поред добро познатог дејства ADK као инхибитора ензима HIV-1-интегразе, ADK испољавају и читав низ различитих биолошких активности. Циљ овог рада било је проучавање ефеката супституције фенилног језгра на особине диоксобутанског дела молекула. Овај структурни фрагмент је одговоран за интеракцију ADK са металним јонима унутар активних места различитих ензима. Утицај pH на структуре девет ADK у воденој средини испитан је помоћу цикличне волтаметрије и диференцијално-пулсне поларографије. За проучавање су изабране само ADK са редокс неактивним метил-супституентима у различитим положајима фенилног језгра и у овом случају је за редокс понашање ADK највише одговоран диоксобутански део молекула. На овај начин систематски је мењан торзиони угао између фенилног прстена и арилне кето групе (Ar-C(O)) и посматран утицај супституената на редокс својства диоксобутанског дела молекула. Стање протонованости ADK на различитим pH вредностима утврђено је из експериментално одређених pK_a вредности. Резултати су показали да у механизмима оксидације и редукције ADK на површини електроде учествује једнак број протона и електрона. Нађене су квантитативне, линеарне корелације између потенцијала редукције и енергија граничних молекулских орбитала и стерних параметара израчунатих за неутрални, моноанјонски и радикал-анјонски облик ADK.

(Примљено 23. новембра 2016, ревидирано 4. фебруара, прихваћено 7. фебруара 2017)

REFERENCES

1. D. J. Hazuda, P. Felock, M. Witmer, A. Wolfe, K. Stillmock, J. A. Grobler, A. Espeseth, L. Gabryelski, W. Schleif, C. Blau, M. D. Miller, *Science* **287** (2000) 646
2. J. S. Wai, M. S. Egbertson, L. S. Payne, T. E. Fisher, M. W. Embrey, L. O. Tran, J. Y. Melamed, H. M. Langford, J. P. Guare, Jr., L. Zhuang, V. E. Grey, J. P. Vacca, M. K. Holloway, A. M. Naylor-Olsen, D. J. Hazuda, P. J. Felock, A. L. Wolfe, K. A. Stillmock, W. A. Schleif, L. J. Gabryelski, S. D. Young, *J. Med. Chem.* **43** (2000) 4923
3. J. J. Tan, C. Liu, H. X. Sun, J. X. Cong, M. L. Hu, X. C. Wang, J. X. Liang, *Mini Rev. Med. Chem.* **12** (2012) 875
4. G. Cuzzuco Crucitti, M. Métifiot, L. Pescatori, A. Messore, V. N. Madia, G. Pupo, F. Saccoliti, L. Scipione, S. Tortorella, F. Esposito, A. Corona, M. Cadeddu, C. Marchand, Y. Pommier, E. Tramontano, R. Costi, R. Di Santo, *J. Med. Chem.* **58** (2015) 1915
5. W. Zhu, Y. Zhang, W. Sinko, M. E. Hensler, J. Olson, K. J. Molohon, S. Lindert, R. Cao, K. Li, K. Wang, Y. Wang, Y.-L. Liu, A. Sankovsky, C. A. F. de Oliveira, D. A. Mitchell, V. Nizet, J. A. McCammon, E. Oldfield, *Proc. Natl. Acad. Sci. U. S. A.* **110** (2013) 123

6. I. V. Krieger, J. S. Freundlich, V. B. Gawandi, J. P. Roberts, V. B. Gawandi, Q. Sun, J. L. Owen, M. T. Fraile, S. I. Huss, J.-L. Lavandera, T. R. Ioerger, J. C. Sacchettini, *Chem. Biol.* **19** (2012) 1556
7. J. Reguera, F. Weber, S. Cusack, *PLoS Pathog.* **6** (2010) e1001101
8. R. M. DuBois, P. J. Slavish, B. M. Baughman, M.-K. Yun, J. Bao, R. J. Webby, T. R. Webb, S. W. White, *PLoS Pathog.* **8** (2012) e1002830
9. K. E. B. Parkes, P. Ermert, J. Fässler, J. Ives, J. A. Martin, J. H. Merrett, D. Obrecht, G. Williams, K. Klumpp, *J. Med. Chem.* **46** (2003) 1153
10. J. Tomassini, H. Selnick, M. E. Davies, M. E. Armstrong, J. Baldwin, M. Bourgeois, J. Hastings, D. Hazuda, J. Lewis, W. McClements, *Antimicrob. Agents Chemother.* **38** (1994) 2827
11. C. Lee, J. M. Lee, N.-R. Lee, B.-S. Jin, K. J. Jang, D.-E. Kim, Y.-J. Jeong, Y. Chong, *Bioorg. Med. Chem. Lett.* **19** (2009) 1636
12. S. Liu, L.-F. Zeng, L. Wu, X. Yu, T. Xue, A. M. Gunawan, Y.-Q. Long, Z.-Y. Zhang, *J. Am. Chem. Soc.* **130** (2008) 17075
13. R. Braga, L. Hecquet, C. Blonski, *Bioorg. Med. Chem.***12** (2004) 2965
14. V. Summa, A. Petrocchi, P. Pace, V. G. Matassa, R. De Francesco, S. Altamura, L. Tomei, U. Koch, P. Neuner, *J. Med. Chem.* **47** (2004) 14
15. L. De Luca, M. L. Barreca, S. Ferro, F. Christ, N. Iraci, R. Gitto, A. M. Monforte, Z. Debyser, A. Chimirri, *ChemMedChem* **4** (2009) 1311
16. B. J. Drakulić, M. Stavri, S. Gibbons, Ž. S. Žižak, T. Ž. Verbić, I. O. Juranić, M. Zloh, *ChemMedChem* **4** (2009) 1971
17. T. Ž. Verbić, B. J. Drakulić, M. F. Zloh, J. R. Pecelj, G. V. Popović, I. O. Juranić, *J. Serb. Chem. Soc.* **72** (2007) 1201
18. T. Ž. Verbić, B. J. Drakulić, M. Zloh, I. O. Juranić, *Lett. Org. Chem.* **5** (2008) 692
19. A. Kuhn, K. G. von Eschwege, J. Conradie, *Electrochim. Acta* **56** (2011) 6211
20. K. C. Kemp, E. Fourie, J. Conradie, J. C. Swarts, *Organometallics* **27** (2008) 353
21. W. C. du Plessis, J. J. C. Erasmus, G. J. Lamprecht, J. Conradie, T. S. Cameron, M. A. S. Aquino, J. C. Swarts, *Can. J. Chem.* **77** (1999) 378
22. M. M. Conradie, A. J. Muller, J. Conradie, *S. Afr. J. Chem.* **14** (2008) 13
23. G. S. Posyagin, E. Y. Posyagina, V. V Zalesov, S. S. Kataev, *Russ. J. Gen. Chem.* **71** (2001) 1574
24. L. Brecker, M. Pogorevc, H. Griengl, W. Steiner, T. Kappe, D. W. Ribbons, *New J. Chem.* **23** (1999) 437
25. M. Huang, W. G. Richards, G. H. Grant, *J. Phys. Chem., A* **109** (2005) 5198
26. T. Ž. Verbić, M. F. Zloh, D. M. Stanković, M. M. Sentić, D. D. Manojlović, I. O. Juranić, in *Proceedings of the* 49th *Meeting of the Serbian Chemical Soc*iety, Kragujevac, Serbia, 2011, p. 16
27. E. P. Serjeant, A. Albert, *The Determination of Ionization Constants: A Laboratory Manual*, *2nd ed.*, Chapman and Hall, London, 1971, p. 44
28. *Gaussian 09, Revision D.01*, Gaussian, Inc., Wallingford CT, USA, 2013
29. O. A. Sof'ina, N. M. Igidov, E. N. Koz'minykh, N. N. Trapeznikova, Y. S. Kasatkina, V. O. Koz'minykh, *Russ. J. Org. Chem.* **37** (2001) 1017
30. H. Beiginejad, D. Nematollahi, M. Noroozi, S. Lotfi, *J. Iran. Chem. Soc.* **12** (2015) 325
31. A. Y. Tesio, S. N. Robledo, H. Fernández, M. A. Zon, *Bioelectrochemistry* **91** (2013) 62
32. E. Gunić, I. Tabaković, K. M. Gaši, D. Miljković, I. Juranić, *J. Org. Chem.* **59** (1994) 1264.